Nigerian Research Journal of Engineering and Environmental Sciences 6(2) 2021 pp. 483-494
p ISSN: 2635-3342; e ISSN: 2635-3350

Nigerian Research Journal of Engineering and Environmental Sciences
Journal homepage: www.rjees.com

Original Research Article

Characterisation of Magnetised and Non-Magnetised Coconut Shell Biochars

***[1]Musa, A., [2]Sani, B.S., [2]Ibrahim, F.B. and [2]Adamu, A.D.**

[1]Department of Chemical Engineering Technology, The Federal Polytechnic, Nasarawa, Nasarawa State, Nigeria.
[2]Department of Water Resources and Environmental Engineering, Ahmadu Bello University, Zaria, Kaduna State, Nigeria.
*abdulmalikmusa44@gmail.com

http://doi.org/ 10.5281/zenodo.5805085

ARTICLE INFORMATION

Article history:
Received 18 Aug, 2021
Revised 27 Sep, 2021
Accepted 03 Oct, 2021
Available online 30 Dec, 2021

Keywords:
Temperature
Biochar
Magnetisation
Magnetised biochar
Physicochemical properties

ABSTRACT

Coconut shell as biomass with little use constitutes a source of pollution. This biomass material was utilized to produce three biochars, CSB400, CSB600 through carbonisation (at 400 and 600 °C), and magnetisation (MCSB600) through the chemical wet co-precipitation method respectively; to assess the effects of temperature and magnetisation on their physicochemical properties. Results showed that temperature decreased the biochar yield from 44.54 to 25.04% for CSB400 and CSB600 respectively. The specific surface area (SSA) increased with temperature from 122.2 to 135 m^2/g while magnetisation (MCSB600) resulted in a 33.81% decrease in SSA compared to its pristine precursor (CSB600). The Fourier transform infrared spectroscopy (FTIR) showed a decrease in functional groups with temperature increase while it increased for magnetised biochar (MCSB600). Results also showed a decrease in both moisture and volatile contents from CSB400 to CSB600 while the ash and fixed carbon contents increased across CSB400 to CSB600 and CSB600 to MCSB600 respectively. The pH increased with carbonisation and magnetisation. Higher cation exchange capacity value, 7.5 cmol/kg was recorded for CSB400 compared to 5.4 cmol/kg for CSB600. The oxygen and carbon contents increased with temperature while the carbon content decreased with magnetisation. The biochars are expected to have different adsorption and soil amendment characteristics based on these variations in the measured properties.

1. INTRODUCTION

A lot of agricultural residues or biomass wastes such as coconut shells and rice husk are produced every year in countries that depend on agriculture as a source of foreign exchange (Paethanom and Yoshikawa, 2012). In 2014, the coconut production in Nigeria was 267,520 tons and this has increased progressively to 290,288 by the year 2019. At present, Nigeria is the 19th producer of coconut in the world (FAOSTAT, 2019).

However, Nigeria still imports about 80% of its domestic coconuts because the demand exceeds the production capacity (Izuaka, 2021). Coconut by-products, especially the shells have little economic value, therefore, end up as solid waste thereby creating secondary pollution. Furthermore, their disposal is not only costly but may also cause environmental problems (Lia *et al*., 2008).

Biochar (BC) is the carbon-rich product produced through the thermochemical conversion of biomass, a carbonisation process in which the content of carbon increases with temperature accompanied by a simultaneous decrease in oxygen and hydrogen contents (Angin *et al*., 2013). Biochar is obtained when for all-purpose and intent, modern (i.e., non-fossil) organic biomass material is charred to obtain a carbon-rich material that is to be used for pollutants removal or carbon sequestration or conditioning of soil (Sani, 2017). Coconut shells are suitable material for biochar production since they contain less amount of ash, more amount of volatile matter and are available at a lower cost in rural areas during all seasons of the year (Sundaram and Natarajan, 2009).

The major constituents of biomass are lignin, cellulose, and hemicellulose (Quaak *et al*.,1999). Biochar is produced mostly from the thermal decomposition of lignin and some extractive parts of biomass, while the volatile matter is transformed into the gas phase and minerals in the biomass are left as ashes (Yang, 2017). This makes it a good source of feedstock in the production of adsorbents that can be used in the remediation of various environmental contaminations (Okafor *et al*., 2012). Biochars can be produced from a range of organic materials under different conditions resulting in products of varying properties (Baldock and Smernik, 2002; Nguyen *et al*., 2004; Asensio *et al*., 2013).

Biochar has great potential for remediation of water contamination due to its fairly large specific surface area, charged surface, and functional groups (Han *et al*., 2015). Biochar is a promising alternative to remedy environments contaminated through adsorption and immobilization of organic and inorganic compounds (Nartey and Zhao, 2014). However, the separation of powdered adsorbents from cleaned environmental matrices is a challenge (Han *et al*., 2015). But with magnetisation of the biochars, through chemical wet co-precipitation method (Safarik *et al*., 1997; Castro *et al*., 2009; Mohan *et al*., 2011; Choi *et al*., 2016; Han *et al*., 2014; Han *et al*., 2015; Juang *et al*., 2018), magnetic separation techniques can be employed to readily separate powdered magnetised adsorbents from treated matrices (Sani, 2017). Magnetised biochars (MBC) have been envisaged to be an alternative route to the recovery of pollutant-loaded adsorbents from cleaned environmental matrices (Han *et al* 2014). However, magnetisation may have changed the sorbent properties, in comparison with the pristine biochars (Han *et al*., 2014). The understanding of its physicochemical properties, which are strongly related to the type of the initial material used and carbonisation conditions, is crucial to identifying the most suitable application for biochar in the environment and thus, information about the production process; heating temperature, and duration is a key factor in defining the most suitable application of biochars (Enders *et al*., 2012; Jindo *et al*., 2014).

The characterisation is crucial in identifying the most suitable application of biochar, thus, information about the production process is a key factor in defining the most suitable application of BCs that will give optimum adsorption capacity (Jindo *et al*., 2014). Biochars produced under different conditions and feedstocks present different physical and chemical properties. Different conditions alter the thermodynamics and kinetics of the pyrolysis and different biomass contain different ratios and forms of cellulose, hemicellulose, lignin, each of which reacts by different pyrolysis mechanisms.

This study was conducted to assess the effects of temperature and magnetisation on the physicochemical properties of coconut shell biochars produced through carbonisation (400 and 600 °C) and magnetised coconut shell biochar produced using chemical co-precipitation magnetisation methods.

2. MATERIALS AND METHODS

2.1. Raw Material and Biochar Preparation

Coconut shells were procured from a fruit vendor at Agoro roundabout, Tudun Wada, Zaria, Kaduna State, Nigeria. The shells were broken into aggregate sizes, washed with running tap water, and then distilled water to remove dirt and impurities before sun drying for about 4-5 days at an ambient temperature of about 28-32 °C. The dried shells were weighed (M_1), loaded in a lid-covered container, and carbonised at 400 and 600 °C in a furnace (Gemco, tlx 59388, Holland) at a heating rate of 10 ±1 °C per minute. The produced biochars were labelled CSB400 and CSB600 respectively. The completely carbonised materials were selected and weighed ($M_{2)}$. The biochars were milled and sieved with 150 and 75 µm meshes to obtain a definite particle size. The powdered biochars were then packed in polyethylene bags and stored in airtight plastic containers. The biochar yield (BCY) was calculated as the ratio of the mass of dry biochar (M_2) to the mass of dry coconut shell (M_1) using Equation (1).

$$BCY = \left(\frac{M2}{M1}\right) \times 100\% \quad (1)$$

2.1.1. Magnetisation of biochar

The wet co-precipitation method reported by Han *et al.* (2014) was adopted with few modifications. An amount (50 g) of pristine biochar (CSB600), 36.6 g of $FeSO_4.7H_2O$, and 66.6 g of $FeCl_3.6H_2O$ were weighed into a beaker with 2000 ml of deionized water stirred and heated to 65 °C on a magnetic stirrer (S/NO5/SS620, Gallenkamp England). The mixture was cooled to below 40 °C and the pH was raised to 10-11 to precipitate the iron hydroxides by adding 5 M NaOH solution dropwise while being stirred. It was stirred for an hour and then allowed to rest overnight. The supernatant was carefully decanted, and the precipitate was rinsed with deionized water and then ethanol with a sorption pump used to drain the remaining moisture and then dried in an oven at 80 °C for 6 hours. The produced magnetised coconut shell biochar was collected with a magnetic rod, weighed, and named MCSB600, after its precursor, CSB600.

2.2. Determination of Specific Surface Area

The specific surface area (SSA) of the biochars were estimated using Sear's method (Sears, 1956), by acidifying 1.5 g of the BC with dilute HCI (dropwise) until the pH was between (3-3.5). Thereafter, 30 g of NaCI was added to the solution while stirring and then made up to 150 ml using distilled water. The solution was titrated with 0.10 M NaOH until the pH reached 9. The volume required to raise the pH from 3.5 to 9 was recorded as the titre value. The procedure was carried out in triplicate and the average titre value was taken. The specific surface areas (m^2/g) were calculated using Equation (2).

$$SSA = 32\,V - 25 \quad (2)$$

Where V is the average volume (ml) of NaOH required to raise the pH of the 1.50 g solution from 3.5 to 9.

2.3. Proximate Analysis

Proximate analysis was conducted according to the American society for testing and materials (ASTM) D3173-75 standard procedures (ASTM, 2002; ASTM, 2007; ASTM, 2008).

2.3.1. Moisture content

The moisture content (MC) of the samples was determined by calculating the loss in weight of the samples with Equation (3) using the hot air oven drying method. A certain amount (1 g) of the sample was measured

in a crucible and heated in the oven for about 1 hour at 105 °C and then cooled in a desiccator (ASTM, 2008).

$$MC\ (\%) = \left(\frac{W2-W3}{W2-W1}\right) \times 100 \quad (3)$$

Where; W_1 is the weight of crucible (g); W_2 is the weight of crucible and sample (g); W_3 is the weight of crucible and sample after heating (g).

2.3.2. Volatile content

The volatile content (VC) of the sample was determined by heating the dried sample in a lid-covered crucible at 600 °C for 6 minutes and then at 900 °C for another 6 minutes (ASTM, 2007). The volatile content is then determined using Equation (4)

$$VC\ (\%) = \frac{W5-W6}{W5-W1} \times 100 \quad (4)$$

Where W_4 is the weight of crucible and sample before oven drying (g); W_5 is the weight of crucible and sample before keeping in a muffle furnace (g); W_6 is the weight of crucible and sample after keeping in a muffle furnace (g).

2.3.3. Ash content

For the ash contents (AC), the residual samples in the crucible were then heated without the lid in a muffle furnace at 750 °C for 30 minutes. The crucibles were then taken out, cooled first in the air, then in desiccators, and weighed (ASTM, 2002). This was repeated until a constant weight was obtained using Equation (5).

$$AC\ (\%) = \frac{W8-W9}{W7-W1} \times 100 \quad (5)$$

Where W_7 is the weight of crucible and sample before oven drying (g); W_8 is the weight of crucible and sample before placing in a muffle furnace (g); W_9 is the weight of crucible and sample after placing in a muffle furnace (g).

2.3.4. Fixed carbon

The fixed carbon (FC) of each sample were calculated by the difference of the sum of moisture, volatile, and ash contents using Equation (6).

$$FC\ (\%) = 100 - \%\ (MC + VC + AC) \quad (6)$$

2.4. Cation Exchange Capacity

Cation exchange capacity (CEC) of the sample was determined using the ammonium saturation method (Udo and Ogunwale, 1986). A 1 M ammonium acetate ($NH_4CH_3CO_2$) saturated solution was prepared by dissolving 77.08 g $NH_4CH_3CO_2$ in distilled water with the mixture cooled, pH adjusted to 7, and then diluted to 1000 ml. A leaching tube was prepared by pouring filter paper pulp on the base plate forming a filter pad. A certain amount (10 g) of air-dried biochar sample was mixed with 20 g of acid-washed silica sand and transferred to a filter pad in the leaching tube. A volumetric flask containing 250 ml of the saturated solution ($NH_4CH_3CO_2$) was inverted into the tube and the rate of leaching was controlled and the leachate was collected. The biochar residue was washed by leaching again with 200 ml of 90% ethanol to remove excess ammonium ion (NH_4^+) and the leachate was discarded. It was leached again using 230 ml of 1 M NaCl into

a 250 ml volumetric flask and the volume made up to 250 ml with the NaCl solution. The concentration of NH_4^+ in the extracted solution was determined and the CEC was calculated using Equation (7).

$$CEC = \frac{25 \times C}{W} \quad (7)$$

Where C is the concentration of NH_4^+(meq/l) in the leachate and W is the weight of biochar used.

2.5. Elemental Analysis

The elemental analysis gives the elemental compositions in terms of carbon (C), hydrogen (H), oxygen (O), and nitrogen (N) contents. The C, H, and N compositions of the materials were determined using a CHN elemental analyser (Flash 2000, Thermo Fisher Scientific Inc., USA) through a high temperature catalysed combustion followed by infrared detection of the generated CO_2, H_2, and NO_2 respectively. The *O* contents were determined by mass balance using Equation (8), assuming the total weight fraction of all measured elements sum up to 1 (100%).

$$O = 100 - \%\ (C + H + N + ash\ content) \quad (8)$$

2.6. Fourier Transform Infrared (FTIR) Spectroscopy

FTIR analysis was carried out on a Cary 630-FTIR (Agilent Technologies Inc., CA) using an adequate amount of the coconut shell feedstock (CSF), CSB400, CSB600, and MCSB600 to detect the various functional groups present. The FTIR spectra were detected within the range of 650-4000 cm^{-1} region.

2.7. Determination of pH

A certain amount of the samples (5 g) was soaked in 30 ml of distilled water (1:6). The mixtures were shaken using a shaker (TT 12F, Techmel USA) for 2 hours and then allowed to stand overnight. The pH values were measured in triplicate with a pH metre (H1991000, Hanna USA) and the average was obtained.

3. RESULTS AND DISCUSSION

3.1. Specific Surface Area

The results presented in Figure 1 showed that the specific surface area increased with the pyrolysis temperature, possibly due to the generation of porosity (Paethanom and Yoshikawa, 2012). The carbonisation temperature increased the specific surface area from 112.6 m^2/g of the coconut shell feedstock to 122.2 m^2/g for CSB400 at 400 °C. As the temperature was increased to 600 °C, the specific surface area increased to 135 m^2/g for CSB600. This could be attributed to the development of more pores due to higher temperatures (Leng, *et al.*, 2021). Similar findings were reported by Yang *et al.* (2016), where the specific surface areas of the biochars generated were 24.33, 46.22, and 76.29 m^2/g for compost carbonised at 300, 500, and 700 °C respectively. The specific surface area decreased by 33.81% from 135 m^2/g of the pristine precursor, CSB600 to 90.1 m^2/g for MCSB600. This was similar to the findings of Oliveira *et al.* (2002) and Han *et al.* (2015). Mohan *et al.* (2011) reported that pores of magnetised carbons contain iron oxides and concluded that the SSA reduction of the magnetised carbons from 733 to 527 m^2/g after iron impregnation could be due to pore blockage by dispersed iron-oxide particles. However, Sani (2017) reported that corresponding pairs of sorbents have comparable values of specific surface area when measured to their carbon content only. Therefore, the SSA of the magnetised pair could be higher than the obtained value if the non-carbonated content was taken into account.

The specific surface area of biochar is a key indicator of the sorption ability of biochar. Correlating the specific surface area with the ash content from Table 1, it can be observed that the ash content did not affect the SSA possibly due to its limited increase, as the specific surface area is often observed to decrease when ash content increases (Arenas and Chejne, 2004) due to blockage or filling of the pores by the ash (Leng, *et al.*, 2021).

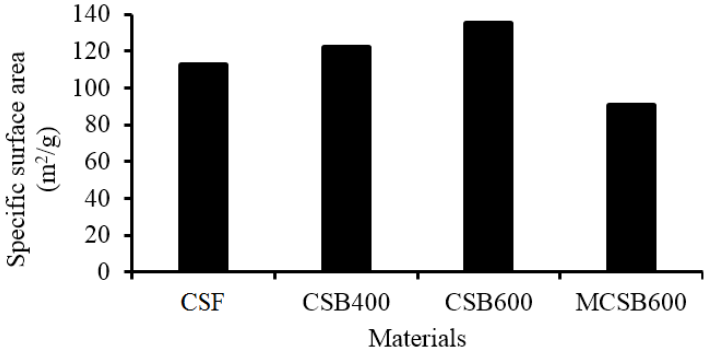

Figure 1: Specific surface area of coconut shell and biochar samples

3.2. Proximate Analysis

The results of the proximate analysis are presented in Table 1. The results showed that biochar yield (Y_{BC}), decreased from 44.54 to 25.04% for the CSB400 and CSB600 respectively. Yang *et al.* (2017) reported similar yields ranging between 21 to 42% and 44 and 40% when mason pine wood and rice straw were carbonised at 350 and 500 °C respectively. The reduction observed could be due volatilization of volatile components of the feedstock such as lignin, cellulose, and hemicellulose at the higher pyrolysis temperature (Nartey and Zhao, 2014). Lignin tends to partially resist decomposition at 400 °C as opposed to hemicellulose and cellulose which decompose at temperatures between 220 to 315 °C and 315 to 400 °C respectively due to different thermal degradation kinetics (Jindo *et al.*, 2014). Ronsse *et al.* (2015) attributed it to the fact that additional secondary char formation occurring at higher temperatures is offset by further devolatilization of the primary char resulting in a diminishing char yield. The ash content increased from 21.00 to 23.08% for CSB400 and CSB600 respectively. However, after magnetisation, the ash content increased sharply to 45.09%. Similar findings were observed by Mohan *et al.* (2011), where ash content increased from 0.50 to 16.93% for the pristine and the magnetised carbons respectively which resulted in the blockage of the pores. It can be observed that the fixed carbon increased as the volatile and moisture contents reduced from 49.36 to 47.06% and 2.18 to 1.86%, respectively with an increase in temperature. An increase in the moisture content for MCSB600 to 1.97% was also observed and this could be due to the attraction of atmospheric moisture or inadequate drying during the magnetisation process as carbon materials are capable of attracting moisture (Alzaydien, 2016).

Table 1: Proximate analysis of coconut shell and biochars

Sample	Moisture content (%)	Ash content (%)	Volatile content (%)	Fixed carbon (%)	Yield (%)
CSF	3.02	18.40	53.70	24.88	nd
CSB400	2.18	21.00	49.36	27.46	44.54
CSB600	1.86	23.08	47.06	28.00	25.04
MCSB600	1.97	45.09	13.52	39.42	nd

nd = not determined

The fixed carbon content which is the combustible carbon that remains after the volatile contents have been expelled increased slightly from 27.46 to 28% with the increase in temperature for CSB400 and CSB600.

The fixed carbon content is considered low when compared to reported literature and this may be attributed to low residence time for carbonisation to take place as similar results were obtained by Sun *et al.* (2016) in their studies on the effect of residence time on biochar properties. However, for the magnetised biochar, fixed carbon appeared to increase to 39.4% for MCSB600 from 28% of its precursor.

3.3. Elemental Analysis

The results of the elemental analysis are presented in Table 2. The result revealed that carbonisation temperature increased carbon (C), from 50.24% of the coconut shell feedstock (CSF) to 58.54% and 56.98% for CSB400 and CSB600 respectively. This is related to increased volatilization of these surface functional group elements during pyrolysis with part of the C could have volatilized into CO_2 or CO (Agrafioti *et al.*, 2013). At the same time, a decrease was recorded for hydrogen (H), (6.0 to 5.98%) while an increase for oxygen (O), (36.98 to 38.22%) with the increase in temperature for CSB400 and CSB600 respectively. The dehydrogenation of CH_3 as a result of thermal induction indicates a change in the biochar recalcitrance (Harvey *et al.*, 2012). In addition, a biomass material typically comprises labile and recalcitrant O fractions; the former is rapidly lost after the initial heating, while the latter is retained in the char of the final product (Rutherford *et al.*, 2012). The nitrogen (N) content, decreased to 2.18% and 2.94% for CSB400 and CSB600 respectively, from 3.12% of the feedstock, CSF. Comparing MCSB600 with its pristine precursor, CSB600, the C content decreased by about 18.41% which corroborates the results from the specific surface area. The H and N decreased from 5.98 to 2.23% and 2.94% and 1.83% respectively.

Table 2: Elemental analysis for the coconut shell and biochars

Sample	C (%)	H (%)	N (%)	O (%)
CSF	50.24	8.60	3.12	36.15
CSB400	58.54	6.00	2.18	36.94
CSB600	56.98	5.98	2.94	38.22
MCSB600	43.40	2.23	1.83	52.54

3.4. Cation Exchange Capacity and pH

The results of the CEC and pH are presented in Figure 2. The CEC is the measure of the surface charge and it decreased from 7.5 to 5.4 cmol/kg for CSB400 and CSB600 respectively. This is similar to the findings of Song and Guo (2012) and Tsai and Chang (2021). The lower CEC of CSB600 could be due to the loss of functional groups at 600 ℃ as CEC of biochar is mainly a result of the acidic surface functional groups (Song and Guo, 2012). The higher the CEC of biochar, the more likely it is to have a better sorption potential for heavy metals. Surface chemistry tends to change with carbonisation temperatures, as the surface functional groups are lost and this can lead to a reduction in the CEC (Song and Guo, 2012; Domingues *et al.*, 2017). This is corroborated by the obtained FTIR results.

The pH of the biochars increased from 7.99 to 8.90 and this may be due to an increase in the basic cations in the ash contents of the biochars (Domingues *et al.*, 2017). The ash content increased from 21 to 23.08% for CSB400 and CSB600 respectively. Tsai and Chang (2021) reported similar findings. Domingues *et al.* (2017), reported that basic cations in ashes are enriched, which may be associated with alkaline species, such as carbonates, oxides, and hydroxides, while acidic surface functional groups are reduced with increasing temperature. Due to magnetisation, the pH of the MCSB600 increased to 9.4 as it can be observed also from Table 1 that the ash content increased from 23.08 to 45.09%. For the MCSB600, the increase in pH of the biochars could also be probably a consequence of the relative concentration of non-carbonised inorganic elements, introduced during magnetisation.

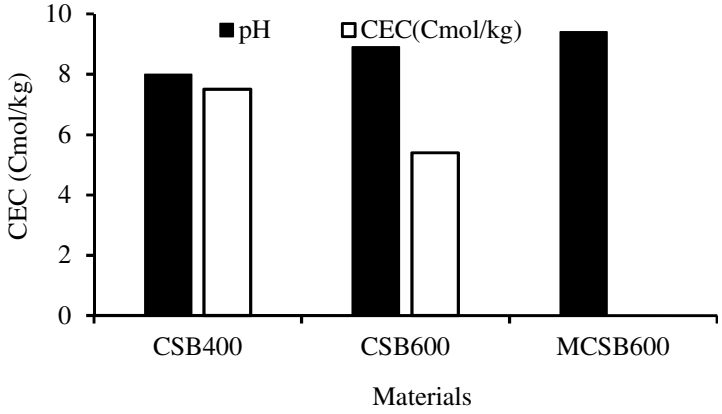

Figure 2: CEC and pH of biochar samples

3.5. Fourier Transform-Infrared Spectroscopy

The FTIR spectra of CSF, CSB400, CSB600, and MCSB600 are presented in Figure 3 and the functional groups they are assigned are listed in Tables 3 to 5. As shown in Tables 3 to 4, there was a loss of functional groups from 18 to 11 as the temperature increased from 400 to 600 °C for CSB400 and CSB600 respectively. Similar losses in functional groups were reported by Jindo *et al.* (2014). The CSB400 contains more alcohol/phenolic and aromatics than CSB600. This could be the reason for CSB400 having a higher CEC value than CSB600. The functional groups increased to 20 as shown in Table 5, for MCSB600 from its pristine precursor (CSB600). This could be due to the presence of iron goethite groups observed around 797.9-898.3 cm^{-1} from the spectra of MCSB600 due to the iron chemicals used during the magnetisation process. The bands at 3324.8-3712.4 cm^{-1} are assigned to the presence of O-H of phenolic/alcohol groups while the bands at 1994.1-2117.1 cm^{-1} are assigned to C≡C of alkynes. The bands at 670.9-913.2 cm^{-1} could be assigned to the presence of C-H of aromatics while at 1661.8-1684.8 cm^{-1} are the alkene (C=C) functional groups. Other bands of anhydride, amine, ether, and nitriles also exist.

Table 3: FTIR peaks assignments of functional groups on CSB400

S/N	Wavelength (cm^{-1})	Bond	Functional group
1	3712.4	O-H	Alcohol/Phenol
2	3619.2	O-H	Alcohol/Phenol
3	3570.8	O-H	Alcohol/Phenol
4	3488.8	O-H	Alcohol/Phenol
5	3339.7	O-H	Alcohol/Phenol
6	2370.6	CO_2	Carbon dioxide
7	2322.1	C≡N	Nitriles
8	2102.2	C≡C	Alkyne
9	1994.1	C≡C	Alkyne
10	1871.1	C=O	Anhydride
11	1684.8	C=C	Alkene
12	1661.8	C=C	Alkene
13	1423.8	N-H	Amine
14	1036.2	C-O	Ether
15	913.2	C-H	Aromatic
16	875.9	C-H	Aromatic
17	745.5	C-H	Aromatic
18	670.9	C-H	Aromatic

Table 4: FTIR peaks assignments of functional groups on CSB600

S/N	Wavelength (cm^{-1})	Bonds	Functional groups
1	3690.1	O-H	Alcohol/phenol
2	3619.2	O-H	Alcohol/phenol
3	3336.0	O-H	Alcohol/phenol
4	2117.1	C≡C	Alkyne
5	1997.9	C≡C	Alkyne
6	1856.2	C=O	Anhydride
7	1684.8	C=C	Alkene
8	1551.8	N-H	Amine
9	1032.5	C-O	Ether
10	872.2	C-H	Aromatic
11	749.2	C-H	Aromatic

Table 5: FTIR peaks assignments of functional groups on MCSB600

S/N	Wavelength (cm^{-1})	Bond	Functional group
1	3857.8	O-H	Alcohol/Phenol
2	3753.4	O-H	Alcohol/Phenol
3	3678.9	O-H	Alcohol/Phenol
4	3634.2	O-H	Alcohol/Phenol
5	3309.6	O-H	Alcohol/Phenol
6	2780.6	H-C=O	Aldehydes
7	2374.3	CO_2	Carbon dioxide
8	2109.7	C≡C	Alkyne
9	1990.4	C≡C	Alkyne
10	1871.1	C=O	Anhydride
11	1804.0	C=O	Anhydride
12	1751.8	C=O	Carboxylic acid
13	1703.4	C=O	Carboxylic acid
14	1561.8	C=C	Alkene
15	1524.5	C=C	Alkene
16	1330.7	N-O	Amine
17	1103.3	C-H	Aromatic
18	1036.2	C-O	Ether
19	898.3	FeO(OH)	Goethite
20	797.7	FeO(OH)	Goethite

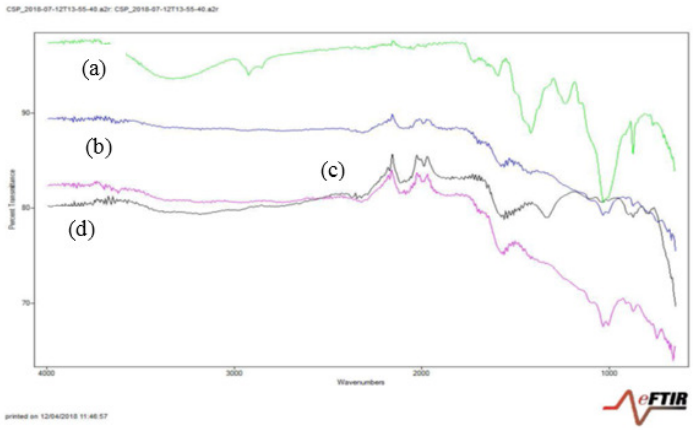

Figure 3: FTIR spectra for (a) CSF, (b) CSB400 (c) CSB600, and (d) MCSB600 respectively

4. CONCLUSION

Carbonisation temperature for the production of the BCs strongly influenced and varied the physicochemical properties from 122.2 to 135 m^2/g, 7.99 to 8.9, and 18 to 11 for the SSA, pH, and functional groups respectively which could affect their sorption performances. Magnetisation resulted in the reduction of the SSA by about 33.18 %, this decrease is attributed to lower carbon content (14.78 %), ash content increased from 23.08 to 45.09 %, pH increased from 8.90 to 9.40 and the functional groups increased from 11 to 20 for the MBC600 compared to its precursor (CSB600). Based on this, it is likely that CSB400 will have a higher sorption capacity for heavy metals while CSB600 could be better for an organic pollutant. It is expected that the sorption potential of MCSB600 could be lowered but not significantly, from its pristine precursor pair, CSB600 in terms of environmental remediation for different contaminants. The biochars are expected to have different adsorption and soil amendment characteristics based on these variations in the measured properties. The results of the study suggest that CSB400 might have better sorption potential for heavy metals while CSB600 and MCSB600 could be better for the sorption of inorganic contaminants.

5. ACKNOWLEDGMENT

The authors wish to acknowledge the assistance of the staff of Environmental Chemistry Laboratory (Department of Water Resources and Environmental Engineering), Soil Chemistry Laboratory (Department of Soil Science), and the Faculty of Science Multiuser Laboratory, all in Ahmadu Bello University, Zaria**,** for their contributions towards the success of this work.

6. CONFLICT OF INTEREST

There is no conflict of interest associated with this work.

REFERENCES

Agrafioti, E., Bouras, G., Kalderis, D. and Diamadopoulos, E. (2013). Biochar production by sewage sludge pyrolysis. *Journal of Analytical and Applied Pyrolysis*, 101, pp. 72–78.

Alzaydien, A.S. (2016). Physical, chemical and adsorptive characteristics of local oak sawdust based activated carbons. *Asian Journal of Scientific Research*, 9(2), pp. 45–56.

ASTM (2002). *Test Method for Ash Content in the Analysis Sample of Coal and Coke* (D3174). Retrieved from: https://www.astm.org/

ASTM (2007). *Test Method for Volatile Matter in the Analysis Sample of Coal and Coke* (D3175). Retrieved from: https://www.astm.org/

ASTM (2008). *Test Method for Moisture in the Analysis Sample of Coal and Coke* (D3173). Retrieved from: https://www.astm.org/

Angin, D., Kose, T.E. and Selengil, U. (2013). Production and characterisation of activated carbon prepared from safflower seed cake biochar and its ability to absorb reactive dyestuff. *Applied Surface Science*, 280, pp. 705–710.

Arenas, E. and Chejne, F. (2014). The effect of the activating agent and temperature on the porosity development of physically activated coal chars. *Carbon*, 42 (2004), pp. 2451–2455.

Asensio, V., Vega, F.A, Andrade, M.L. and Covelo, E.F. (2013). Tree vegetation and waste amendments to improve the physical condition of copper mine soils. *Chemosphere*, 90(2), pp. 603-610.

Baldock, J.A. and Smernik, R.J. (2002). Chemical composition and bioavailability of thermally altered Pinus Resinosa (Red Pine) wood, *Organic Geochemistry*, 33(9), pp. 1093-1109.

Bolan, N.S., Adriano, D.C. and Mahimairaja, S. (2004). Distribution and bioavailability of trace elements in livestock and poultry manure by-products. *Critical Reviews in Environmental Science and Technology*, 34(3), pp. 291–338.

Brownsort, P.A. (2009). Biomass pyrolysis Processes: A review of scope, control and variability; UKBRC Working Paper 5; UK Biochar Research Centre: Edinburgh, UK.

Castro, C.S., Guerreiro, M.C., Goncalves, M., Oliveira, L.C.A. and Anastácio, A.S. (2009). Activated carbon/iron oxide composites for the removal of atrazine from aqueous medium. *Journal of Hazardous Materials*, 164(2-3), pp. 609–614.

Choi, Y., Wu, Y., Sani, B., Luthy, R. G., Werner, D. and Kim, E. (2016). Performance of retrievable activated carbons to treat sediment contaminated with polycyclic aromatic hydrocarbons. *Journal of Hazardous Materials*, 320, pp. 359–367.

Domingues, R.R., Trugilho, P.F., Silva C.A., Melo, I.C.N.A.d., Melo, L.C.A., Magriotis, Z.M. (2017). Properties of biochar derived from wood and high-nutrient biomasses with the aim of agronomic and environmental benefits. *PLoS ONE*, 12(5), e0176884.

Enders, A., Hanley K., Whitman T., Joseph S. and Lehmann, J. (2012). Characterization of biochars to evaluate recalcitrance and agronomic performance. *Bioresource Technology*, 114, pp. 644–653.

Food and Agriculture Organization (FAO). (2019). Food and Agriculture Organization Corporate Statistical Database (FAOSTAT). Retrieved from: http://www.fao.org/faostat/en/search/coconut.

Han, Z., Sani, B., Mrozik, W., Obst, M., Beckingham, B., Karapanagioti, H.K. and Werner, D. (2014). Magnetite impregnation effects on the sorbent properties of activated carbons and biochars. *Water Research*, 70(0), pp. 394–403.

Han, Z., Sani, B., Akkanen, J., Abel, S., Nybom, I., Karapanagioti, H. and Werner, D.A. (2015). A critical evaluation of magnetic activated carbon's potential for the remediation of sediment impacted by polycyclic aromatic hydrocarbons. *Journal of Hazardous Materials*, 286(0), pp. 41–47.

Harvey, O.M., Herbert, B.E., Kuo, L.J. and Louchouarn, P., (2012). Generalized two-dimensional perturbation correlation Infrared spectroscopy reveals mechanisms for the development of surface charge and recalcitrance in plant-derived biochars. *Environmental Science and Technology*, 46(19), pp. 10641–10650.

Izuaka, M. (2021). Nigerian coconut market worth over $6 billion–Minister. *Premium Times*. Retrieved from: https://www.premiumtimesng.com/news/more-news/466516-nigeria-coconut-market-worth-over-6-billion-minister.html

Jindo, K., Mizumoto, H., Sanchez-Monedero, M.A., Sawada, Y. and Sonoki, T. (2014). Physical and chemical characterisation of biochars derived from different agricultural residues. *Biogeosciences*, 11(23), pp. 6613–6621.

Juang, R., Yei, Y., Liao, C., Lin, K. and Lu, H. (2018). Synthesis of magnetic Fe_3O_4/activated carbon nanocomposites with high surface area as recoverable adsorbents. *Journal of the Taiwan Institute of Chemical Engineers*, 90, pp. 51–60.

Leng, L., Xiong, Q., Yanga, L., Li, H., Zhou, Y., Zhanga, W., Jiang, S. and Li, H., Huang., H. and Li, H., and Huang., H. (2021). An overview on engineering the surface area and porosity of biochar. *Science of the Total Environment*, 763, pp. 144204.

Lia, W., Yang, K, Peng, J., Zhang, L., Guo, S. and Xia, H. (2008). Effects of carbonisation temperatures on characteristics of porosity in coconut shell chars and activated carbons derived from carbonised coconut shell chars. Industrial Crops and Products, 28(2), pp. 190–198.

Mohan, D., Sarswat, A., Singh, V. K., Alexandre-Franco, M. and Pittman, C.U. (2011). Development of magnetic activated carbon from almond shells for trinitrophenol removal from water. *Chemical Engineering Journal*, 172(2–3), pp. 1111–1125.

Nguyen, T.H, Brown R.A. and Ball, W.P. (2004). An evaluation of thermal resistance as a measure of black carbon content in diesel soot, wood char and sediment. *Organic Geochemistry*, 35(3), pp. 217-234.

Novak, J.M., Lima, I., Xing, B., Gaskin, J.W., Steiner, C., Das, K.C., Ahmedna, M., Rehrah, D., Watts, D.W., Busscher, W.J. and Harry, S., (2009). Characterization of designer biochar produced at different temperatures and their effects on a loamy sand. *Annals of Environmental Science*, 30(3), pp. 195–206.

Nartey, O. D. and Zhao, B.W. (2014). Biochar preparation, characterization, and adsorptive capacity and its effect on the bioavailability of contaminants: An overview. *Advances in Materials Science and Engineering*, 2014, pp. 1–12.

Okafor, P.C, Okon, P.U, Daniel, E.F. and Ebenso, E.E. (2012). The adsorption capacity of coconut (*Cocos nucifera L.*) shell for lead, copper, cadmium and arsenic from aqueous solutions. *International Journal Electrochemistry Science*, 7(12), pp. 12354–12369.

Oliveira, L.C.A., Rios, R.V.R.A., Fabris, J.D., Garg, V., Sapag, K. and Lago, R.M. (2002). Activated carbon/iron oxide magnetic composites for the adsorption of contaminants in water. *Carbon*, 40(12), pp. 2177–2183.

Paethanom, A. and Yoshikawa K. (2012). Influence of pyrolysis temperature on rice husk char characteristics and its tar adsorption capability, *Energies*, 5(12), pp. 4941–4951.

Quaak, P., Knoef, H. and Stassen, H.E. (1999). *Energy from biomass: A review of combustion and gasification technologies*. Washington, D.C.: World Bank.

Ronsse, F., Nachenius, R. W. and Prins, W. (2015). *Carbonization of biomass*. In: Pandey, A., Bashkar, T., Stocker, M., and Sukumaran, R. (Eds.) Recent advances in thermochemical conversion of biomass (pp. 293–323).

Rutherford, D. W., Wershaw, R. L., Rostad, C. E. and Kelly, C. N. (2012). Effect of formation conditions on biochars: compositional and structural properties of cellulose, lignin, and pine biochars. *Biomass Bioenergy*, 46, pp. 693–701.

Safarik, I., Lunackova, P., Mosiniewicz-Szablewska, E., Weyda, F. and Safarikova, M. (2007). Adsorption of water-soluble organic dyes on ferrofluid modified sawdust. *Water Research and Technology*, 61(3), pp. 247–253.

Sani, B.S. (2017). *Modelling of pollutant adsorption by activated carbon and biochar with and without magnetite impregnation for the treatment of refinery and other wastewaters*. (Doctoral thesis, Newcastle University). Retrieved from https://thesis.ncl.ac.uk/dspace/bitstream/10443/3595/1/Sani%2C B.S. 2017.pdf.

Sears, G.W. (1956). Determination of specific surface area of colloidal silica by titration with sodium hydroxide. *Analytical Chemistry*, 28(12), pp. 1981–1983.

Song, W. and Guo, M. (2012). Quality variations of poultry litter biochar generated at different pyrolysis temperatures. *Journal of Analytical and Applied Pyrolysis*, 94, pp. 138–145.

Sun, J., He, F., Pan. Y. and Zhang, Z. (2016). Effects of pyrolysis temperature and residence time on physicochemical properties of different biochar types. *Acta Agriculturae Scandinavica, Section B – Soil & Plant Science*, 67(1), pp. 12–22.

Sundaram, E.G. and Natarajan, E. (2009). Pyrolysis of coconut shell: An experimental investigation. *The Journal of Engineering Research*, 6(2), pp. 33–39.

Tsai, C.-C. and Chang, Y.F. (2021). Quality evaluation of poultry litter biochar produced at different pyrolysis temperatures as a sustainable management approach and its impact on soil carbon mineralization. *Agronomy*, 11(9), pp. 1692.

Udo, E.J. and Ogunwale, J.A. (1986). Laboratory manual for analysis of soil, plant and water samples. University of Ibadan, Nigeria.

Yang, G., Wu, L., Xian, Q., Shen, F., Wu, J. and Zhang, Y. (2016). Removal of congo red and methylene blue from aqueous solutions by vermicompost-derived biochars. *PLoS ONE*, 11(5), pp. 1–18.

Yang, X., Wang H., Strong P.J, Xu S., Liu S., Lu K., Sheng K., Guo J., Che L., He L., Ok Y.S, Yuan G., Shen Y. and Chen X., (2017). Thermal properties of biochars derived from waste biomass generated by agricultural and forestry sectors, *Energies*, 10(4), pp. 469.